Pergamon

PII: S0022-3697(96)00015-7

J. Phys. Chem Solids Vol 57, No. 10, pp. 1473–1477, 1996

0022-3697/96 $15.00 + 0.00

PRETRANSITIONAL CONDENSATION IN MIXED FERROELECTRICS

J. TOULOUSE and R. K. PATTNAIK
Physics Department, Lehigh University, Bethlehem, PA 18015, U.S.A.

(*Received* 12 *June* 1995; *accepted* 14 *August* 1995)

Abstract—We report the observation of a condensation of polar clusters in the mixed ferroelectric system, $KTa_{1-x}Nb_xO_3$ (KTN) approximately 20 K above the transition for Nb concentrations between 1.2% and 30%. This condensation is marked by a 'reduced softening' of the bulk susceptibility, a downward shift of the transition temperature, the appearance of a coercive field and of odd harmonics in the polarization. In KTN this condensation can be described by a modified Landau–Ginzburg model. Such a condensation should be a feature common to many mixed ferroelectrics and has also been observed in mixed ferroelastics.

Keywords: D. ferroelectricity, D. dielectric properties, D. anharmonicity, D. lattice dynamics, D. phase transitions.

1. INTRODUCTION

Ferroelectric materials with substitutional impurities, known as mixed ferroelectrics, have been the focus of fundamental research by several groups [1, 2]. In many of these, the impurity occupies an off-center position in the unit cell [3] while its counterpart in the host unit cell stays centered. As a result, a local field is induced, one of the interesting consequences of which is the formation of polar clusters surrounding the impurities. One of the earliest evidence of this local field-induced effect was provided by Müller *et al.* [4] who used EPR to study the mixed system, $KH_2CR_xAs_{1-x}O_4$ and reported spectra of lower symmetry in the high temperature paraelectric phase. Dalal *et al.* [5] and Ribeiro *et al.* [6] have reported similar measurements on doped KDP. Results obtained with other microscopic techniques such as nqr and nmr were reviewed by Blinc [7]. Borsa and coworkers [8] reported the observation of a cusp in the susceptibility of the ferroelectric $K_{1-x}Li_xTaO_3$ (KLT), which they interpreted as ordering of random-site electric dipole in non-polar lattice. In all the above systems the condensation discussed was a 'condensation/freezing' process taking place in the vicinity of individual impurities and leading to the formation of polar clusters. For instance, in KLT, it is strictly due to the large local deformation that accompanies the substitution of individual Li for K; it occurs far above the transition and is not a cooperative effect. This was clearly demonstrated in a previous Raman study [9] of the hard optic mode in KLT. In this study, the TO_2 polar optic mode was shown to appear at approximately 200 K for all Li concentrations. Closer to T_c, a detailed analysis of the TO_2 lineshape indicated the presence of polar nanoregions with linear dimensions of about 35 Å [10, 11]. In $KTa_{1-x}Nb_xO_3$ (KTN), polar clusters, similar to those in KLT, should be found at higher temperatures also leading, through their mutual interactions, to the formation of polar nanoregions at lower temperatures. Such polar clusters and nanoregions in KTN have indeed also been evidenced through the observation of the TO_2 polar optic mode [12, 13]. Their presence has also been confirmed through dielectric, polarization and NMR measurements. However, in the present communication, we show that the mechanism by which these polar regions form is very different in KTN and in KLT. Our previous Raman study of KTN [9] revealed a sharp increase in the integral intensity of the TO_2 line starting approximately at $T_c + 20$ K for all Nb concentrations where T_c is strongly dependent on the Nb concentration. These relationships between the condensation and ferroelectric temperature suggest a cooperative character for the condensation. Here we report dielectric and polarization results which suggest that the condensation of polar clusters is itself a transition driven by the interaction of the soft polar mode with several neighboring clusters leading to the formation of polar nanoregions and changes in the system dynamics including a departure from the Curie–Weiss behavior of the dielectric susceptibility.

2. THEORY

Several authors [14–20] have addressed the theoretical aspects of a local condensation around substitutional impurities. In particular, Schmidt and Schwab

[15, 16], using a Landau–Ginzburg model, have shown that the condensation can be described as a local ordering. According to them the free energy functional can be expanded in the local order parameter $\phi(x)$ as

$$F(\phi) = (2v)^{-1} \int \mathrm{d}^3x \Big\{ a\phi^2(x) + \frac{b}{2}\phi^4(x) + c(\nabla\phi)^2 + U(x)\phi^2(x) \Big\}. \quad (1)$$

Here v is the volume considered, $a(T)$, b, and c are the usual Landau expansion coefficients of the pure system and $U(x)$ describes the influence of the impurities and must be negative (i.e. attractive) in order to induce a condensation. In the present case, the impurities of the model correspond to the clusters in the specific KTN case, and the origin of this last term is most likely electrostriction. Using Euler variational principle subject to the constraint of a constant total intensity of fluctuation, and ignoring the non-linear term, the total free energy $F(\phi)$ can be minimized to yield an expression [15] for the average bulk susceptibility χ:

$$a(T)\phi(x) - (c\nabla^2 + |U(x)|)\phi(x) = \chi^{-1}\phi(x). \quad (2)$$

The second term on the LHS represents the average cluster contribution, $\chi_{\mathrm{cl}}^{-1}(T)$ such that $\chi^{-1} = a(T) - \chi_{\mathrm{cl}}^{-1}$. This last expression indicates that a local transition or polar condensation can take place when $a(T^*) - \chi_{\mathrm{cl}}^{-1}(T^*)$. Assuming the usual Curie–Weiss dependence, $a(T) = (1/C)(T - T_0)$, the condensation temperature can be obtained:

$$T^* = T_0 + C\chi_{\mathrm{cl}}^{-1} > T_0. \quad (3)$$

It is important to note that, in the original model of Schmidt and Schwabl which described a purely local condensation, C represented the Curie–Weiss constant of the pure system. In the present application of the model, however, we shall see that the results justify taking C as the Curie–Weiss constant of the doped system thus supporting the notion of cooperative condensation. We also note that, in the model, due to finite range of the attractive interaction potential, $U(x)$, χ_{cl} only contributes to the bulk susceptibility in the vicinity of each cluster. As a result χ is not expected to diverge but, at most, to pass through a maximum at T^*, where the correlation length of the order parameter is $\sim\sqrt{(c\chi_{\mathrm{cl}})}$. We shall return to these two points in the discussion. For $T < T^*$, the local condensate or polar nanoregion reduces the susceptibility of the local order parameter thereby contributing to a downward shift in the bulk transition temperature. Also below T^*, the non-zero local order parameter, ϕ_0 should contribute to the non-linearities of the system and, in particular, to the third harmonic in the field induced polarization through the $b\phi^4$ term in eqn (1).

In the experimental evidence presented below, the condensation of polarization is manifested in:

1. a departure of the Curie–Weiss like response of the bulk susceptibility and reduced softening; and
2. the appearance of a remnant polarization, a coercive field and harmonics in the polarization response of the system.

3. DIELECTRIC RESULTS AND DISCUSSION

The dielectric measurements on KTN samples with Nb concentration ranging from 1.2 to 30% were made with a HP-4194A Impedance/Gain-Phase Analyzer.

Since the dielectric responses are largely similar at all concentrations of Nb, we first discuss the results of the 15.7% sample in detail and later summarize the results for the other samples. In Fig. 1(a) we present

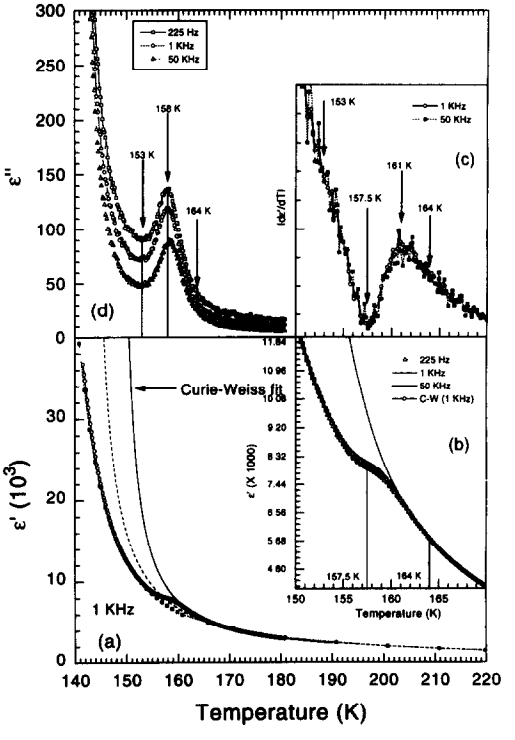

Fig. 1. Real and imaginary dielectric constants of KTN-15.7% sample as a function of temperature at 1 kHz. (a) Reduced dielectric softening and deviation from Curie-Weiss response, (■ - -) before application of any bias field (see text), (O –) after the application of bias field (see text). (b) data and fit on expanded temperature scale. (c) temperature derivative of ϵ' showing the region of reduced softening starting with the condensation at 161 K. (d) imaginary part, ϵ'', showing a peak in the same temperature region.

the results of two sets of measurements of the dielectric constant, $\epsilon'(\nu, T)$, taken at 1 KHz in the temperature range 140–220 K. In this figure, the set with solid markers corresponds to data taken earlier, before application of d.c. bias fields. In the following however, we primarily focus on the data taken later (open markers) leaving the comparison to the end. At high temperatures, the susceptibility is accurately described by a Curie–Weiss law [21, 22]:

$$\epsilon'(T) = \frac{C}{T - T_0} + \epsilon_0, \tag{4}$$

where C is the Curie constant, T_0 the Curie–Weiss temperature, and ϵ_0 is a temperature independent or background dielectric constant. The frequency dependence of ϵ' is illustrated in Fig. 1(b) where we compare the results of measurements at three different frequencies on an expanded temperature scale. As shown in Fig. 1(b) for the 15.7% crystal and several frequencies, the dielectric constant departs from the Curie–Weiss law in a narrow range of temperature near 164 K. This departure we qualify as 'reduced softening'. As a result of this departure, T_c is found 9 K below the Curie–Weiss temperature, T_0, for this crystal. The derivative $d\epsilon'/dT$, shown in Fig. 1(c), is helpful in identifying the important temperatures in the process and in particular the two inflection points at ~161 and ~157.5 K and the change in curvature at 164 and 153 K. This figure also confirms the absence of a frequency dependence in the frequency range of the dielectric measurements.

In Fig. 1(d) we present the imaginary part of the dielectric constant, which closely parallels the behavior of ϵ', with a first inflection point near 161 K, a peak at 158 K, a minimum at 153 K and only a small frequency dependence of these temperatures ($\leqslant 1$ K) between 500 and 1 MHz.

Dielectric constant measurements were also made on samples of other concentrations, and the real part was fitted with eqn (4). For all concentrations, it was found to display a Curie–Weiss-like behavior in the high temperature region, but to depart from it at T^* while approaching the condensation. In Table 1 below, we present a summary of the parameters obtained from fitting the dielectric data at 1 KHz for different concentrations.

It is fundamental to emphasize that χ_{cl}^{-1} has been calculated from eqn (3) using the Curie–Weiss constant, C obtained from the fit [eqn (4)] at high temperature and clearly influenced by the presence of Nb impurities as seen in Table 1. As pointed out earlier this procedure is at odds with the original application of Schmidt and Schwabl's model [15] in which C was taken to be the Curie–Weiss constant of pure $KTaO_3$. Nevertheless the constancy of $\chi_{cl}^{-1}(T^*)$ for all the concentrations studied would appear to justify this new application of the model and support the cooperative nature of the condensation. It is further interesting to note that the value of χ_{cl} (~5000) is close to the experimental value of the dielectric constant obtained just above the condensation [see Fig. 1(a)]. According to the model, this figure can be interpreted as the average value of the cluster susceptibility that is necessary in order to trigger the condensation of a fraction of the clusters into nanoregions. The constancy of χ_{cl} is a rather remarkable result that is particularly well illustrated by the two series of measurements made on the 15.7% crystal before and after application of large d.c. bias fields. T_c was found to be the same for these two series and, even though C and T_0 had changed, χ_{cl} is nevertheless found to remain constant. We hypothesize that, as a result of the large fields, the distributions of cluster sizes has been modified with no change, however, in the volume fraction of the crystal occupied by clusters. Besides the constancy of χ_{cl}^{-1}, the two most significant points to be noted in Table 1 are that: (1) the dielectric constant, ϵ', departs from a Curie–Weiss law approximately 20 K above the transition for all concentrations (the variations observed do not present any meaningful trend and are due to error bars in the fitting to the C–W law); and (2) the actual transition temperature, T_c, is shifted down from the Curie–Weiss T_0 by 6–10 K.

Because a Curie–Weiss law is due to dynamic

Table 1. Summary of the various parameters obtained from fitting eqn (4) to the data

Conc.	C(K)	T_0	T_c	T^*	χ_{cl}^{-1}
$KTaO_3$*	50,000	13	—	—	—
1.2% (a)	59,915.6	20.2	12.21	33.8	2.3e-4
1.2% (b)	60,473	19.6	12.15	32	2.05e-4
3%	63,848	66.4	59.5	80	2.13e-4
15%	100,202	133.5	129	152	1.84e-4
15.7% (1)	116,520	143	139	164	1.8e-4
15.7% (2)	84,447	148.4	139	164	1.8e-4
30%	119,670	230.4	224	258.6	2.39e-4

*See Ref. [21].

(a) and (b) refer to two different samples, and (1), and (2) refer to measurements before and after application of large d.c. bias fields.

fluctuations of the polarization, it is natural to interpret the departure noted in point (1) above as a suppression of these fluctuations due to the condensation of polar clusters into polar nanoregions which are known to exist near but above T_c [9]. This departure, and the downward shift of the transition temperature that accompanies it, are in fact predictions of the theoretical model outlined earlier.

Also according to Schmidt and Schwabl's model [15[, the polar nanoregions should possess a net polarization that is dependent on non-linear (order parameter) interactions. Measurements of polarization hysteresis shall then show the passage from linear to non-linear (hysteresis) loops accompanying the condensation of polar clusters into nanoregions. In the following section we present polarization measurements on the KTN-15.7% sample and discuss the results.

4. POLARIZATION HYSTERESIS RESULTS AND DISCUSSION

Polarization measurements as a function of both temperature and excitation frequency were made using a Sawer–Tower circuit with a peak a.c. field of 1000 V/cm and the experiment was done upon cooling. In Fig. 2(a) we present the polarization hysteresis loops obtained with the KTN-15.7% sample at different temperatures across the condensation range. Two significicant features in the loops are worth noting. First, the loops at the higher temperatures are simple ovals (or linear) while at lower temperatures they become non-linear, particularly on the down field part of each half cycle. The oval loops are simply the result of a phase lag between the excitation field and the polarization of the dynamic clusters. The non-linear loops, by contrast, reveal strong interactions between clusters having coalesced into polar regions. These strong interactions also explain the rising coercive field shown in Fig. 2(b). Here again the condensation process is seen to begin between 165 and 163 K.

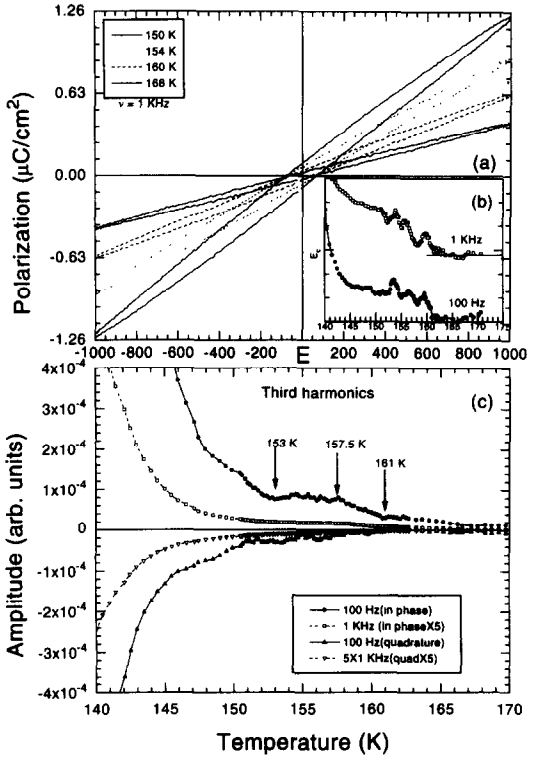

Fig. 2. (a) Hysteresis loops of KTN-15.7% at different temperatures. Above 160 K the loops are oval while below have an "S" (non-linear) shape. (b) Step increase in the coercive field at 160 K showing onset of strongly interacting polar nanoregions. (c) Third harmonic of the excitation derived from a Fourier analysis of the polarization signal. It is evident that the cubic (non-linear) term begins to increase with the condensation of the polar nanoregions at $T_c + 20$ K.

In order to characterize more precisely the polarization non-linearities, i.e. find the frequency components, we have Fourier analyzed the measured polarization signal (that consisted of 500 data points per trace). The amplitude of the third harmonic is shown in Fig. 2(c) as a function of temperature for two different frequencies. It rises near 164 K and is approximately constant between 157.5 and 153 K before increasing again at lower temperatures. The low amplitude tail extending above 164 K is a field induced effect and the effect of the condensation is reduced at higher frequencies or higher fields.

5. SUMMARY AND FINAL REMARKS

In summary, we have observed in the $KTa_{1-x}Nb_xO_3$ (KTN) system the condensation of polar custers into polar regions approximately 20 K above the ferroelectric transition temperature for all the Nb concentrations. This condensation is evidenced by a reduced softening of the bulk susceptibility, departing from the conventional Curie–Weiss response, and a concurrent peak in the imaginary dielectric constant. It is also evidenced by the appearance of non-linearities and a rising coercive field in the polarization response. This condensation marks the beginning of strongly correlated fluctuations between niobium ions within the polar nanoregions.

Several general remarks can now be made about the above results and the condensation process that they reveal. As was mentioned, earlier NMR measurements [12, 13] on KTN, and even measurements on one of the present samples, have shown that the off-centering of a fraction of Ta ions takes place at temperatures much above the present condensation temperature. At these same temperatures Raman spectra begin to show broad single phonon lines normally forbidden in the cubic phase and indicative

of the appearance of dynamical clusters. The present dielectric and polarization results suggest that, due to the soft phonon mode, or equivalently the high polarizability of the lattice, near neighbor clusters begin to interact strongly near T^* to form polar nanoregions. The very small frequency dependence of the experimental features observed would itself suggest the cooperative nature of the condensation process. However, none of the experimental observations reflect the divergence of the correlation length or the susceptibility. In the original application of Schmidt and Schwabl's model, this is simply due to the finite range of the impurity potential, $U(x)$. In the present case we can offer a more specific explanation. In disordered ferroelectrics such as KTN, it has been shown that the random dipoles interact directly via the normal dipole–dipole interaction but also indirectly via the lattice through the Lorentz field, with only the latter leading to ferroelectric ordering [23]. This provides a simple explanation for the absence of a divergence while still allowing for the cooperative character of the condensation. At intermediate distances, of the order of the size of the polar nanoregions, ferroelectric interactions dominate while, at large distances, it is the direct dipole–dipole interaction that dominate, preventing an indefinite growth of the correlation length of the polarization.

A very similar behavior has been observed by Salje and co-workers [24, 25] in the mixed ferroelastic crystal $Pb_3(P_{1-x}As_xO_4)_2$. In these, the condensation is itself marked by a second peak in the specific heat, distinct from the main peak that marks the ferroelastic transition. Such a condensation transition above the structural transition should be generic to many disordered ferroelectric systems.

Acknowledgements—We thank L. A. Boatner for providing the samples. We also acknowledge helpful discussions with B. E. Vugmeister, L. A. Knauss and Phil DiAntonio. This work was supported by Office of Naval Research Grant No. N00014-90-J-4098.

REFERENCES

1. Vugmeister B. E. and Glinchuk M. D., *Rev. Mod. Phys.* **62,** 938 (1990).
2. Höchli U. T., Knorr K. and Loidl A., *Adv. Phys.* **39,** 405 (1990).
3. Yacoby Y., *Phys. Rev.* **B44,** 6700 (1991).
4. Müller K. A., Dalal N. S. and Berlinger W., *Phys. Rev. Lett.* **36,** 1504 (1976).
5. Dalal N. S., Blinc R., Prelovšek P. and Reddoch A. H., *Solid State Commun.* **43,** 887 (1982).
6. Ribeiro G. M., Gonzaga L. V., Chaves A. S., Gazinelli R., Blinc R., Cevc P., Prelovšek P. and Silikin N. I., *Phys. Rev.* **B25,** 311 (1982).
7. Blinc R., *Ferroelectrics* **16,** 33 (1977).
8. Borsa F., Höchli U. T., van der Klink J. J. and Rytz D., *Phys. Rev. Lett.* **45,** 1884 (1980).
9. Toulouse J., DiAntonio P., Vugmeister B. E., Wang X. M. and Knauss L. A., *Phys. Rev. Lett.* **68,** 232 (1992).
10. Uwe H., Lyons K. B., Crater H. L. and Fleury P. A., *Phys. Rev.* **B33,** 6463 (1986).
11. Toulouse J., Wang X. M., Knauss L. A. and Boatner L. A., *Phys. Rev.* **B43,** 8297 (1991).
12. van der Klink J. J., Rod S. and Châtelain A, *Phys. Rev.* **B33,** 2084 (1986).
13. Rod S. and van der Klink J. J., *Phys. Rev.* **B49,** 470 (1994).
14. Höck K. H. and Thomas H., *Z. Physik.* **B27,** 267 (1977).
15. Schmidt H. and Schwabl F., *Phys. Lett.* **61A,** 476 (1977).
16. Schmidt H. and Schwabl F., *Z. Physik.* **B30,** 197 (1978).
17. Levanyuk A. P., Osipov V. V., Sigov A. S. and Sobyanin A. A., *Sov. Phys. JETP* **49,** 176 (1979).
18. Levanyuk A. P. and Sigov A. S., *Defects and Structral Phase Transitions.* Gordon and Breach, NY (1988) and references therein.
19. Fisher B. and Klein M. W., *Phys. Rev. Lett.* **37,** 756 (1976).
20. Vugmeister B. E. and Glinchuk M. D., *Sov. Phys. JETP* **52,** 482 (1980).
21. Lines M. E. and Glass A. M., *Principles and Applications of Ferroelectrics and Related Materials.* Clarendon Press, Oxford (1979).
22. Jona F. and Shirane G., *Ferroelectric Crystals.* Dover Publications, New York (1993).
23. Toulouse J., Vugmeister B. E. and Pattnaik R., *Phys. Rev. Lett.* **73,** 3467 (1994).
24. Salje E., Devarajan V., Bismayer U. and Gumaraes D. M. C., *J. Phys. C: Solid State Phys.* **16,** 5233 (1983).
25. Salje E. and Wruck B., *Phys. Rev.* **B28,** 6510 (1983).